

## Energetics and structures of aluminum-lithium clusters

Hai-Ping Cheng, R. N. Barnett, and Uzi Landman

*School of Physics, Georgia Institute of Technology, Atlanta, Georgia 30332*

(Received 23 February 1993)

Energetics and structures of small aluminum-lithium clusters were investigated using structure-minimization and dynamic simulated annealing on the electronic Born-Oppenheimer surface, calculated via the local-spin-density-functional method in conjunction with nonlocal pseudopotentials. It is suggested that evolutionary patterns of electronic structure, energetics, and binding in  $\text{AlLi}_n$  clusters may be analyzed within a framework where atomic-based characteristics, associated mainly with closing of the Al  $3p$  shell, dominate for  $n \leq 5$ , while a perturbed delocalized electronic cluster-shell pattern, containing an  $\text{AlLi}_5$  "core," develops for larger clusters (i.e., for  $n \geq 6$ ). The ground-state electronic and geometrical structures of  $\text{AlLi}_n$  clusters, as well as those of  $\text{Al}_2\text{Li}_{10}$  which may be viewed as two slightly distorted  $\text{AlLi}_5$  units bonded to each other, are discussed.

### I. INTRODUCTION

Size-dependent evolutionary patterns of energetics, thermodynamics, stability (abundance), spectroscopy, collective excitations, structure, reactivity, and fission barriers and dynamics of metal clusters are currently the subject of intensive experimental and theoretical investigations.<sup>1</sup> Many of these studies, particularly for small and medium size free-electron metal clusters, were analyzed in the framework of the cluster electronic shell model (CSM), developed first in the context of the spherical jellium model,<sup>2</sup> where the valence electrons contributed by the constituent atoms are regarded as delocalized (effectively screening the ionic potentials) over a homogeneously distributed positive background. The CSM, which was extended<sup>2(a),3</sup> to account for deformations from spherical symmetry and emerges also in calculations where the discreteness of the ions is maintained,<sup>4-6</sup> introduces an electronic shell structure, where  $n_e$  electrons ( $n_e = n_A Z_A$ , where  $Z_A$  is the atomic valency and  $n_A$  the number of atoms in the cluster) fill the orbitals  $|nl\rangle$  according to the pattern (for a homonuclear cluster)  $1s^2|1p^6|1d^{10}2s^2|1f^{14}|2p^6|, \dots$ , where the vertical bars indicate the largest shell-closing discontinuities at  $n_e^* = 2, 8, 20, 34, 40, \dots$  electrons. Accordingly, shell closing at the above "magic numbers" would be reflected in drops in the ionization potentials (IP) and atomic binding energies (and thus abundance in the mass spectrum) upon crossing a shell-closing boundary.

The electronic shell structure of metal clusters has been observed experimentally and theoretically calculated and analyzed for elemental clusters [mainly for alkali, alkaline-earth, and group IIIa (boron and aluminum) metals], as well as for some mixtures of alkali and alkali/alkaline-earth metals.<sup>2(a),4</sup> For heteroclusters one of the central questions is the extent to which the CSM picture is preserved in such systems.<sup>7</sup> Since the CSM implies delocalization of the electrons over the ion cores (and consequently relative insensitivity to geometrical structure), one may expect deviations from the patterns predicted via CSM whenever localized bonds and/or

large structure-sensitive crystal-field splittings may occur.

In this communication we show that while in heteroclusters composed of alkali metals and those made of alkali and closed-shell alkaline-earth metals, behavior according to the CSM is observed<sup>4</sup> [with possible reordering of the levels,<sup>7,8</sup> the physical picture for alkali clusters containing an open-shell heteroatom (e.g.,  $\text{AlLi}_n$ ) may be different<sup>9-11</sup>]. Our results<sup>10</sup> indicate that the nature of bonding in  $\text{AlLi}_n$  clusters may be viewed as changing from a localized atomic (or molecular)-like one for  $n \leq 5$  to a perturbed delocalized one for  $n > 5$ , containing an  $\text{AlLi}_5$  "core." Furthermore, the equilibrium state of the  $\text{Al}_2\text{Li}_{10}$  cluster may be described as composed of two  $\text{AlLi}_5$  units bound to each other. In Sec. II we provide pertinent calculational details, and our results are given in Sec. III.

### II. METHOD

The method used in our investigation consists of electronic structure calculations of the ground-state Born-Oppenheimer (BO) potential energy of the system via a self-consistent solution of the local-spin-density (LSD)-functional Kohn-Sham (KS) equations, coupled with classical molecular dynamics (MD) of the ions (BO-LSD-MD method;<sup>6</sup> see Ref. 12 for a detailed description of the method). Norm-conserving ionic pseudopotentials constructed according to the procedure in Ref. 13 are used in our calculations with the  $p$  component taken as local, and  $s$ -component nonlocality is treated via the Kleinman-Bylander construction<sup>14</sup> performed in real space.<sup>12</sup> The operations of the Hamiltonian on the wave functions are performed using a dual-space method (i.e., fast Fourier transforms are used to calculate the action of the kinetic-energy operator in momentum space). In solving the KS-LSD equations (using an iterative matrix diagonalization method<sup>12</sup>) the spin degrees of freedom are unrestricted. In our method the ionic system is not replicated (that is, no supercell is used) and large calculational grids were taken to assure convergence of the plane-wave basis set (typically a cutoff of the plane-wave kinetic energy of 15

Ry was used).

The optimal structures and corresponding energies which we present were determined for the smaller clusters (e.g.,  $\text{AlLi}_n$ ,  $n \leq 5$ ) via steepest-descent-like minimization starting from several judiciously chosen structures, and by dynamic simulated annealing (DSA) for the larger ones (in the DSA simulations the clusters were heated to  $\sim 1300$  K and then cooled, via inclusion of a damping term in the ionic equations of motion, at an average rate of  $10^{14}$  K/s). The classical equations of motion were integrated using a fifth-order Gear predictor-corrector algorithm, with a time step of  $5 \times 10^{-15}$  s.

### III. RESULTS

Calculated ground-state structures of  $\text{AlLi}_n$  ( $1 \leq n \leq 8$ ) clusters and of  $\text{AlLi}_{17}$  are shown in Figs. 1(a) and 1(b), respectively. We observe first that while for homonuclear  $\text{Li}_n$  clusters two-dimensional ground-state clusters prevail up to  $n \leq 6$  (see Ref. 4), for  $\text{AlLi}_n$  clusters the equilibrium structures are three dimensional for  $n \geq 3$ . We also note that for  $n \leq 5$  the aluminum atom does not occupy an internal position, while for larger clusters it is internally located, surrounded by Li atoms although not necessarily at equal distances from all of them. The cal-

culated equilibrium internuclear bond length is  $5.35 \pm 0.02$  a.u. in the  $\text{AlLi}$  molecule, and the average Al-Li distance between the Al atom and the nearest Li atoms decreases upon addition of lithiums to the cluster (see Table I).

The atomization energies ( $E_b/n$ ), relative stability  $\Delta E_n = E(\text{AlLi}_n) - E(\text{AlLi}_{n-1}) - E(\text{Li})$ , vertical ionization potentials  $\text{IP} = E(\text{AlLi}_n) - E(\text{AlLi}_n^+)$ , and spin multiplicities ( $2S+1$ ) for the parent neutral and ionic clusters are given in Table II, and the corresponding valence-electron KS energy levels (for the neutrals) are shown in Fig. 2. First we note (Table I) the monotonic increase in both  $E_b/n$  and  $-\Delta E_n$  for  $1 \leq n \leq 5$  which drop at  $n=6$  (more pronounced in  $\Delta E_n$ ), indicating unique stability of the 8-valence electron  $\text{AlLi}_5$  cluster. The ionization potentials for  $1 \leq n \leq 5$  exhibit only a mild variation (note the absence of a clear odd-even pattern), also decreasing sharply for  $n > 5$ .

On first sight one may conclude that the above trends indicate electronic cluster-shell closing at  $\text{AlLi}_5$  (8-valence electrons) in accord with the CSM. However, inspection of the energy-level diagram (Fig. 2) shows that the lowest eigenvalue (originating from the Al 3s level) is well separated from the higher lying ones. This by itself is not contradictory to the CSM prediction, since the opening of a large gap between the s and p manifolds may

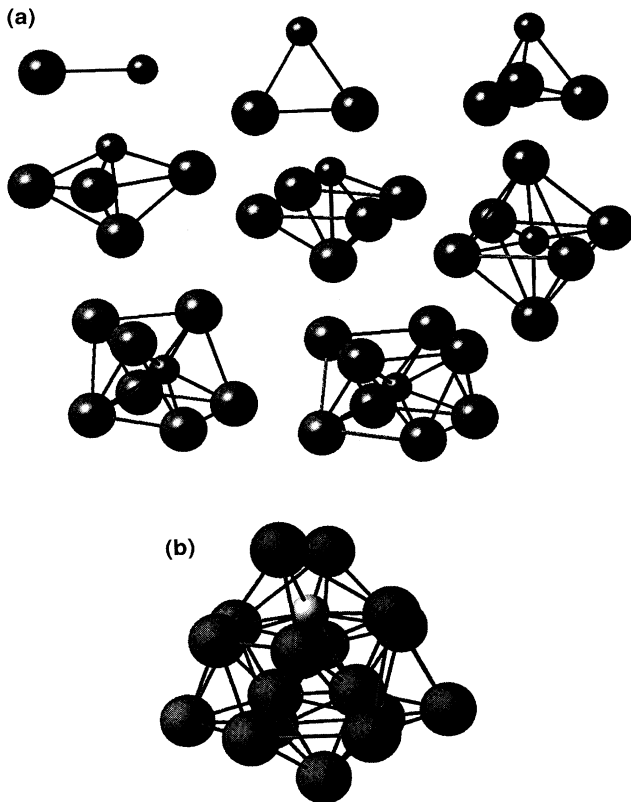


FIG. 1. (a) Ground-state structures of  $\text{AlLi}_n$  ( $1 \leq n \leq 8$ ) clusters. For structural parameters, see Table I. Large and small spheres represent Li and Al atoms, respectively. (b) Ground-state structure of  $\text{AlLi}_{17}$ . The structure is of  $C_2$  symmetry. Large spheres represent Li atoms, and the small sphere corresponds to the Al atom.

TABLE I. Al-Li distances  $d(\text{Al-Li})$  in the equilibrium structures of  $\text{AlLi}_n$  clusters. In case of several equal Al-Li distances, the number of such Al-Li pairs appears as a multiplicative integer in front of the corresponding distance. All distances are in a.u. with an estimated accuracy of  $\pm 0.02$  a.u. In the third column the symmetry of the structure is given. Clusters which distort from the ideal symmetric structure are indicated by an asterisk. For  $\text{AlLi}_3$  the calculated high-spin (see Table II) ground-state structure is slightly distorted from the indicated ideal  $C_{3v}$  symmetry, with two of the (Al-Li) distances taking the value 4.95 a.u. and the third one a value of 5.06 a.u. For  $\text{AlLi}_8$  we give the (Al-Li) distances calculated for the cluster constrained to  $D_{4d}$  symmetry. However the structure obtained via simulated annealing (with no constraint on the symmetry) is distorted from the ideal  $D_{4d}$  symmetry with the energy lowered by 0.2 eV with respect to the symmetric structure. For  $\text{AlLi}_7$ , four  $d(\text{Al-Li})$  distances are given; with reference to the structure of the cluster given in Fig. 1(a), the first distance is to the Li atom at the upper left corner, the next is to the other two Li atoms at the upper face, the third is to the two Li atoms at the bottom face (left), and the last is to the two other Li atoms at the bottom face. The structure of  $\text{AlLi}_7$  resembles that of  $\text{AlLi}_8$  (see Fig. 1) with one Li atom missing on the upper face.

$n$	$d(\text{Al-Li})$	Symmetry
1	5.35	$C_{\infty v}$
2	(2 × 5.22)	$C_{2v}$
3	(3 × 4.98)	$C_{3v}^*$
4	(2 × 4.82, 2 × 4.89)	$C_{2v}$
5	(4 × 4.74, 5.13)	$C_{4v}$
6	(6 × 4.58)	$O_h$
7	(4.70, 2 × 4.85, 2 × 4.74, 2 × 4.81)	$C_{1h}$
8	(8 × 4.82)	$D_{4d}^*$

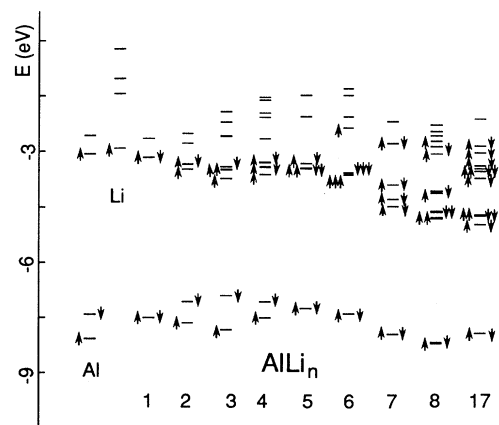


FIG. 2. Energies, in eV, of Kohn-Sham spin orbitals, obtained via spin-unrestricted LSD calculations, for structurally optimized clusters. Results are shown for Al, Li, and  $\text{AlLi}_n$  ( $n=1-8, 17$ ). Up and down arrows indicate the electron-spin occupancy (in case of degeneracy only one level is drawn, and when no arrows are drawn the orbital is unoccupied).

be attributed to the strong attraction by the  $\text{Al}^{+3}$  ion. However, the electronic distributions of the lowest and, in particular, the highest occupied eigenvalues in  $\text{AlLi}_5$ , which are of  $s$  and  $p$  character (see Ref. 15, and caption to Fig. 3), do not show a delocalized character, with the electronic charge excluding the regions about the lithiums [see Figs. 3(c) and 3(d), top row]. Additionally, bonding in the cluster is covalent in nature, characterized by charge accumulation in the regions connecting the Al and Li ions [Fig. 3(b), top].

One may consider an alternative electron-counting scheme, where only the electron in the  $3p$  level of the aluminum atom participates in the electronic shell structure of the cluster. However the consequent prediction that  $\text{AlLi}_7$  is a “magic number” cluster is not supported by the pattern of binding energies and ionization potentials (Table II). The above, coupled with the absence of a marked gap between the highest occupied orbitals of  $\text{AlLi}_7$  and  $\text{AlLi}_8$ , which would have constituted a signature of shell closing in  $\text{AlLi}_7$ , and the separation in  $\text{AlLi}_7$  between the highest occupied state and the triplet of states below it, reflected also in a delocalized nature of the former [see Fig. 3(d), bottom], leads us to discard this electron-counting scheme as one underlying a CSM behavior. In this context note the marked delocalization

of the electronic distribution corresponding to the top-most occupied orbital in  $\text{AlLi}_7$ , shown in Fig. 3(d) (bottom), which is 80%  $s$  and 18%  $d$  (Ref. 15), compared to the markedly localized nature of the  $p$ -like orbital (97%  $p$ ) corresponding to the second highest occupied state, shown in Fig. 3(c) (bottom).

We suggest that the evolution of the electronic structure in  $\text{AlLi}_n$  clusters may be conveniently analyzed within a framework where clusters with  $n \leq 5$  are viewed as largely influenced by localized atomic, rather than delocalized CSM, considerations, and that the characteristics of shell-closing in  $\text{AlLi}_5$  are associated mainly with closing of the Al  $3p$  electronic manifold, albeit somewhat perturbed by the lithium environment via hybridization, bonding, and crystal-field effects. We further suggest that upon addition of Li atoms to the  $\text{AlLi}_5$  “core,” a delocalized perturbed CSM pattern evolves with the ordering of the  $1d$  and  $2s$  levels reversed from that corresponding to homonuclear jellium clusters (i.e., for our system the  $2s$  is below the  $1d$ , see Ref. 7). We note, however, the significant degree of  $2s$ - $1d$  mixing due to crystal-field effects. As an illustration we show in Fig. 2 the level scheme for  $\text{AlLi}_{17} \equiv (\text{AlLi}_5)\text{Li}_{12}$  [see structure in Fig. 1(b), where the Al occupies an internal but noncentral position], exhibiting the development of a six-level  $sd$  shell, which while of delocalized  $sd$  character, is perturbed by the lower-lying aluminum-based  $s$  and  $p$  atomiclike core, to which it must be orthogonal, as well as by crystal-field effects.<sup>16</sup>

The above picture of the energetics of  $\text{AlLi}_n$  clusters and the special role of  $\text{AlLi}_5$  in it suggests that  $\text{Al}_n\text{Li}_{5n}$  clusters, at least for some values of  $n \geq 2$ , may exhibit structures and energetics characteristic of assembly of such clusters from  $\text{AlLi}_5$  units. This idea is somewhat related to the proposal that certain crystalline materials structures could be assembled from small, stable, cluster units<sup>17</sup> (for example, a solid fullerene may be regarded as an assembly of fullerene molecules, e.g.,  $\text{C}_{60}$  clusters, bonded together via van der Waals interactions<sup>18</sup>).

While work pertaining to the above proposal is still in progress we show in Figs. 4 and 5 the ground-state structure and KS energy levels for  $\text{Al}_2\text{Li}_{10}$ , determined via DSA (see Sec. II). As seen from Fig. 4 this cluster is made of two slightly distorted  $\text{AlLi}_5$  units, bonded to each other. This structure possesses a center of inversion (i.e.,  $S_2$  symmetry) at the midpoint of the Al-Al “bond” (the distance between the two Al atoms in  $\text{Al}_2\text{Li}_{10}$  is 5.67 a.u., compared to 5.18 a.u. in the  $^3\Pi_u$  ground state of the  $\text{Al}_2$  molecule, whose calculated binding energy is 1.91 eV, in agreement with recent density-functional calculations

TABLE II. Energetics of  $\text{AlLi}_n$  structurally optimized clusters.  $E_b/n$  is the atomization energy per number of Li atoms, IP is the vertical ionization potential,  $\Delta E_n = E(\text{AlLi}_n) - E(\text{AlLi}_{n-1})$ , and  $(2S+1)$  is the spin multiplicities for neutral  $\text{AlLi}_n$  clusters and their ions ( $n, i$ ), respectively. Energies in eV.

$n$	1	2	3	4	5	6	7	8	17
$E_b/n$	1.24	1.34	1.48	1.58	1.69	1.62	1.59	1.57	1.56
IP	5.37	5.44	5.45	5.22	5.19	3.67	4.10	4.13	4.13
$-\Delta E_n$	1.24	1.45	1.74	1.91	2.11	1.29	1.59	1.46	
$(2S+1)$	(1,2)	(2,3)	(3,4)	(2,1)	(1,2)	(2,1)	(1,2)	(2,1)	(1,2)

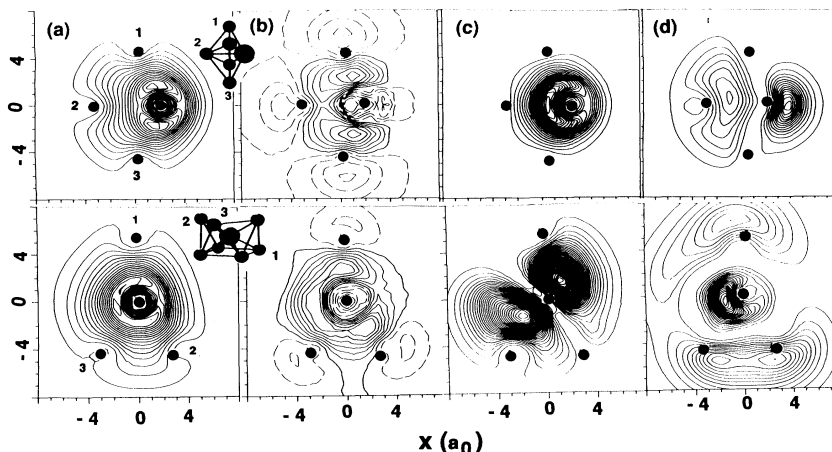


FIG. 3. Contours of total electronic charge distribution (a), difference between the total distribution in the cluster and the superposition of atomic charge densities [in (b) solid and dashed contours indicate charge accumulation and depletion, respectively], and charge distributions in individual orbitals (c) and (d). Results in the top row are for  $\text{AlLi}_5$  and at the bottom row for  $\text{AlLi}_7$ . For  $\text{AlLi}_5$  the contours in (c) and (d) correspond to the lowest and highest occupied orbitals of  $s$  (94%  $s$ , 5%  $p$ ) and  $p$  (7%  $s$ , 88%  $p$ , 3%  $d$ ) character, respectively, when the spherical harmonics analysis (Ref. 15) is based on the charge-density center [the corresponding values when the Al atom is taken as the origin are the same for the  $s$ -like orbital and (14%  $s$ , 75%  $p$ , 11%  $d$ ) for the  $p$ -like one]. For  $\text{AlLi}_7$  the contours in (c) and (d) correspond to the second highest and topmost occupied orbitals, which are of localized  $p$  (1%  $s$ , 97%  $p$ , 1%  $d$ ) and delocalized  $s$ - $d$  (80%  $s$ , 1%  $p$ , 18%  $d$ ) character, respectively, when calculated with respect to the centroid of the electronic charge density (very similar results are obtained when the analysis is performed with the Al ion taken as the origin). The structures of the clusters [see Fig. 1(a)] are shown in the insets (large and small spheres corresponding to Al and Li atoms, respectively). The  $\text{AlLi}_5$  contours are in the plane containing the Al ion and the three Li ions marked by numbers. The  $\text{AlLi}_7$  contours are in the plane containing, approximately, the Al ion and the three numbered Li ions. In the insets giving the structures of the clusters [see also Fig. 1(a)] the large sphere represents the Al atom and the smaller spheres correspond to Li atoms. In the contour plots, solid dots indicate the locations of the ions, or their projections on the contour plane.

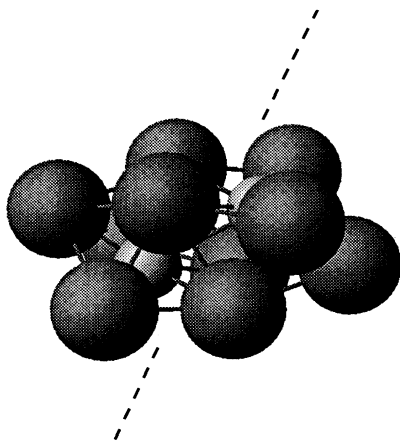


FIG. 4. Ground-state structure of  $\text{Al}_2\text{Li}_{10}$ . Large dark spheres represent Li atoms, and the two small lighter spheres inside the structure correspond to the Al atoms. The structure can be viewed as composed of two  $\text{AlLi}_5$  subunits (left and right of the inclined dividing plane normal to the plane of the figure, indicated by the dashed line) bonded along the square bases of the subunits [compare to Fig. 1(a) where the equilibrium structure of  $\text{AlLi}_5$  is given]. In  $\text{Al}_2\text{Li}_{10}$  the Al atom in each of the  $\text{AlLi}_5$  subunits is closer to the four base Li atoms than in the equilibrium structure of  $\text{AlLi}_5$ , and the capping Li atom in each subunit is displaced from its more symmetrical location in the ground-state structure. The structure is of  $S_2$  symmetry, with the center of inversion in the middle of the Al-Al bond.

of  $\text{Al}_n$  clusters<sup>19</sup>.

The KS eigenvalue spectrum of  $\text{Al}_2\text{Li}_{10}$  shown in Fig. 5, and the correlation between it and that corresponding to  $\text{AlLi}_5$ , reflect the nature of bonding in the cluster, which does not follow a conventional cluster-shell-model description (rather, it is reminiscent of bonding between two closed-shell atoms or molecules). We also find that the excess binding energy ( $E[\text{Al}_2\text{Li}_{10}] - 2E[\text{AlLi}_5]$ ),

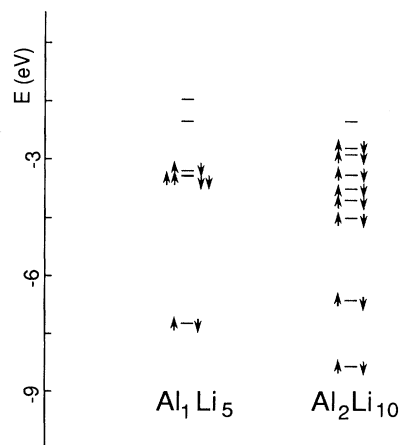


FIG. 5. Energies (in eV) of Kohn-Sham spin orbitals, obtained via LSD calculations, for the ground-state structures of  $\text{AlLi}_5$  and  $\text{Al}_2\text{Li}_{10}$ .

gained by bringing together the two  $\text{AlLi}_5$  units to form the  $\text{Al}_2\text{Li}_{10}$  cluster, is 2.66 eV.

#### IV. SUMMARY

The ground-state electronic and geometrical structures of  $\text{AlLi}_n$  clusters were investigated using local-spin-density-functional calculations and dynamic simulated annealing. The structures are three dimensional for  $n \geq 3$ , and for  $n \leq 5$  the Al atom is located externally (that is, not surrounded by Li atoms), while for  $n \geq 6$  the Al atom occupies an internal position, although not necessarily at the center of the cluster.

Based on analysis of the energetics (see Table II and Fig. 2) and electronic charge distributions for  $\text{AlLi}_n$  clusters ( $1 \leq n \leq 8$  and  $n = 17$ ) we propose that the size evolutionary patterns of the properties of  $\text{AlLi}_n$  clusters can be described in terms of a scheme where closing of the Al  $3p$  shell dominates for  $n \leq 5$ , while a perturbed hybridized and delocalized electronic cluster-shell pattern, contain-

ing an  $\text{AlLi}_5$  core, develops for larger clusters.

Motivated by our interpretation of the properties of  $\text{AlLi}_n$  clusters and their size-dependent evolution, we suggest that  $\text{Al}_n\text{Li}_{5n}$  aggregates (at least for some values of  $n \geq 2$ ) may exhibit properties characteristic to an assembly of such clusters from  $\text{AlLi}_5$  subunits. Our results for the smallest member of the above sequence, i.e.,  $\text{Al}_2\text{Li}_{10}$ , show that the ground-state structure and nature of bonding in this cluster can indeed be correlated with two  $\text{AlLi}_5$  units bonded to each other.

#### ACKNOWLEDGMENTS

This research was supported by the U.S. Department of Energy (DOE) AG05-86ER45234. Computations were performed on Cray YMP computers at the National Energy Research Supercomputer Center, Livermore, California, and the Florida State Supercomputer Center, supported by grants from the DOE, and at the Pittsburgh Supercomputer Center.

<sup>1</sup>See review by U. Landman, R. N. Barnett, C. L. Cleveland, and G. Rajagopal in *Physics and Chemistry of Finite Systems*, edited by P. Jena, S. N. Khanna, and B. K. Rao (Kluwer, Dordrecht, 1992), Vol. 1, p. 165, and other articles therein.

<sup>2</sup>(a) See review by W. A. de Heer, W. D. Knight, M. Y. Chou, and M. L. Cohen, *Solid State Phys.* **40**, 93 (1987); (b) W. E. Ekaradt, *Phys. Rev. B* **29**, 1558 (1984).

<sup>3</sup>W. E. Ekaradt and Z. Penzar, *Phys. Rev. B* **38**, 4273 (1988).

<sup>4</sup>See review by V. Bonacic-Koutecky, P. Fantucci, and J. Koutecky, *Chem. Rev.* **91**, 1035 (1991).

<sup>5</sup>U. Rothlisberger and W. Andreoni, *J. Chem. Phys.* **94**, 8129 (1991).

<sup>6</sup>R. N. Barnett, U. Landman, and G. Rajagopal, *Phys. Rev. Lett.* **67**, 3058 (1991).

<sup>7</sup>C. Baladron and J. A. Alonso, *Physica B* **154**, 73 (1988), and references therein.

<sup>8</sup>U. Rothlisberger and W. Andreoni, *Chem. Phys. Lett.* **198**, 478 (1992).

<sup>9</sup>We are not aware of experimental data on  $\text{AlLi}_n$  clusters. For a recent experimental study of  $\text{Al}_n\text{Na}_m$  for  $n = 2-26$  and  $1 \leq m \leq 3$ , see A. Nakajima *et al.*, *J. Chem. Phys.* **95**, 7061 (1991).

<sup>10</sup>Previous calculations for  $\text{AlLi}_n$  limited to  $1 \leq n \leq 4$  were performed by B. K. Rao and P. Jena, *Phys. Rev. B* **37**, 2867 (1988). The optimal geometries and energies reported in that paper differ from our results.

<sup>11</sup>For a preliminary account of our work, see H.-P. Cheng, R. N. Barnett, and U. Landman, *Z. Phys. D* (to be published).

<sup>12</sup>R. N. Barnett and U. Landman *Phys. Rev. Lett.* **70**, 1775 (1993); Details of the method are given in R. N. Barnett and U. Landman, *Phys. Rev. B* (to be published).

<sup>13</sup>N. Troullier and J. L. Martins, *Phys. Rev. B* **43**, 1993 (1991). The cutoff radii used in the construction of the pseudopotentials are 2.1 a.u. and 2.5 a.u. for  $s$  and  $p$ , respectively, in Al; 2.2 a.u. and 2.8 a.u. for  $s$  and  $p$ , respectively, in Li.

<sup>14</sup>L. Kleinman and D. Bylander, *Phys. Rev. Lett.* **48**, 1425

(1982).

<sup>15</sup>The angular momentum character is calculated via analysis of the KS wave functions of the  $i$ th occupied state in spherical harmonics, i.e.,

$$\psi_i(\mathbf{r}) = \sum_{l,m} \phi_{lm}^i(r) Y_{lm}(\Omega), \quad (1)$$

with the weight of the  $(l,m)$  component given by  $w_{l,m}^i = \int [\phi_{lm}^i(r)]^2 r^2 dr$ . We performed such analyses with the expansion in Eq. (1) centered about the electronic charge center of the  $\text{AlLi}_n$  clusters or, alternatively, taking the Al atom as the origin.

<sup>16</sup>For  $\text{AlLi}_{17}$  (a 20-valence electron cluster) spherical harmonics analysis<sup>15</sup> of the occupied KS levels yields  $s^{1.96}$  for the  $2e$  in the lowest occupied level and  $s^{0.39} p^{4.71} d^{0.64}$  for the  $6e$  in the next three occupied levels, when based on the Al atom taken at the origin. The centroid of the total electronic charge distribution is displaced relative to the Al ion by 2.7 a.u. We also note that the centroid of the electronic charge density corresponding to the four lowest occupied KS orbitals is displaced by 2.2 a.u. from the aluminum ion while that corresponding to the six highest occupied KS orbitals is located further away from the Al ion at a distance of 3.2 a.u. Analysis for the six highest occupied KS levels, centered about the charge-density centroid of the cluster, yields  $s^{1.29} p^{0.03} d^{0.56}$  for the  $2e$  in the lowest KS orbital in this manifold and a total of  $s^{0.56} p^{0.79} d^{8.1} f^{0.25}$  for the  $10e$  in the next highest five occupied orbitals. These results indicate  $3s$  and  $3p$  levels localized about the Al, and a higher-in-energy delocalized and hybridized  $sd$  shell (with the KS orbital energy of the  $s$ -like component of the shell lying below that of the  $d$ -like component).

<sup>17</sup>S. N. Khanna and P. Jena, *Phys. Rev. Lett.* **69**, 1664 (1992).

<sup>18</sup>A. F. Hebard, in *Physics and Chemistry of Finite Systems* (Ref. 1), p. 1213, and references therein.

<sup>19</sup>R. O. Jones, *Phys. Rev. Lett.* **67**, 224 (1991).